Inflammatory macrophages prevent colonic goblet and enteroendocrine cell differentiation through Notch signaling

Roger Atanga[1], Aaron S. Romero[1], Anthony Jimenez Hernandez[1], Eduardo Peralta-Herrera, Seth D. Merkley[1], *Julie G. In[1,2], and *Eliseo F. Castillo[1,2]

[1] Division of Gastroenterology and Hepatology, Department of Internal Medicine, University of New Mexico Health Sciences, Albuquerque, NM.

[2] Autophagy Inflammation and Metabolism Center of Biomedical Research Excellence, University of New Mexico Health Sciences, Albuquerque, NM.

*Correspondence

Email: Ecastillo@salud.unm.edu

Email: Jgin@salud.unm.edu

1 University of New Mexico

Division of Gastroenterology and Hepatology

Department of Internal Medicine

University of New Mexico Health Sciences Center

Albuquerque, NM 87131, USA.

505-272-5703

Short title: Inflammatory macrophages activate Notch signaling

Keywords: Macrophages, Colitis, Goblet cells, enteroendocrine cells, organoids, Notch

Abstract

Inflammatory macrophages in the intestine are a key pathogenic factor driving inflammatory bowel disease (IBD). Here, we report the role of inflammatory macrophage-mediated notch signaling on secretory lineage differentiation in the intestinal epithelium. Utilizing IL-10-deficient ($Il10^{-/-}$) mice, a model of spontaneous colitis, we found an increase in Notch activity in the colonic epithelium as well as an increase in intestinal macrophages expressing Notch ligands, which are increased in macrophages upon inflammatory stimuli. Furthermore, a co-culture system of inflammatory macrophages and intestinal stem and proliferative cells during differentiation reduced goblet and enteroendocrine cells. This was recapitulated when utilizing a Notch agonist on human colonic organoids (colonoids). In summary, our findings indicate that inflammatory macrophages upregulate notch ligands that activate notch signaling in ISC via cell-cell interactions, which in turn inhibits secretory lineage differentiation in the gastrointestinal (GI) tract.

Introduction

Notch signaling is a cell-cell communication mechanism important for many aspects of biology, including intestinal stem cell (ISC) differentiation[1,2]. This process mainly occurs through signal-sending cells expressing Notch ligands that bind Notch receptors on signal-receiving cells. There are 5 mammalian Notch ligands (Delta-like: DLL1, DLL3, and DLL4; and Serrate (Jagged)-like: Jagged1 and Jagged2) and 4 Notch receptors (Notch1–4)[2]. Notch activation occurs after i) Notch ligand binds a Notch receptor resulting in proteolysis of the extracellular domain of Notch receptor by the metalloprotease ADAM10[3] and ii) the mechanical pull of Notch ligand on the Notch receptor. The Notch intracellular domain (NICD) is then released into the cytosol by the γ-secretase complex. The cytosolic NICD translocate to the nucleus binding the transcription factor CSL (CBF-1 /Suppressor of Hairless/ Lag-1) resulting in the expression of numerous target genes such as *Hes1* (Hairy and enhancer of split 1) and *Hey1* (Hes related family bHLH transcription factor with YRPW motif 1) that mediate Notch activity[1,2,4]. During ISC differentiation, continuous Notch signaling through *Hes1* and *Hey1* expression represses the transcription factor *Atoh1* (atonal bHLH transcription factor 1) to promote absorptive cellular differentiation, *e.g*., enterocytes in small intestine and colonocytes in the colon [4-6]. Whereas, certain secretory cells, like goblet and enteroendocrine cells, are promoted through the inhibition of Notch signaling and the expression of *Atoh1* [7-9]. Nevertheless, both absorptive and secretory cells are critical to the epithelial barrier to maintain intestinal homeostasis.

Intestinal macrophages also contribute to ISC renewal, homeostasis, and differentiation, as depletion of macrophages reduces stem cell numbers and impairs cellular differentiation [10]. Macrophages are abundant in the intestine and act as a first line of defense in the gut. Unlike other tissue macrophages, intestinal macrophages exhibit an anti-inflammatory phenotype and display high phagocytic and bactericidal activity, as well as a high tolerance towards foreign material [11,12]. However, in states of chronic intestinal inflammation, like Crohn's disease (CD) and ulcerative colitis (UC) the two major forms of inflammatory bowel disease (IBD), an accumulation of inflammatory macrophages can be observed in the mucosa [13,14]. The influence of inflammatory macrophages on ISC differentiation is unclear but macrophages have been found to be

both Notch signal-sending and signal-receiving cells. Interestingly, Notch signaling is dysregulated in IBD[5,15-18]. Nevertheless, it is unclear which cell-type promotes increased Notch signaling in IBD. Herein, we show intestinal macrophages in the inflamed colon of a mouse model of IBD display increased expression of Notch ligands Jagged1 and DLL3. The inflamed colon also showed increased levels of Notch target gene expression and reduced levels of *Atoh1*. We further show inflammatory macrophages prevent secretory cell differentiation while anti-inflammatory macrophages promoted goblet and enteroendocrine cell differentiation. This was recapitulated in human organoids in the absence of macrophages and through the utilization of a Notch agonist. In summary, our findings indicate that inflammatory macrophages can inhibit secretory lineage differentiation in the gastrointestinal (GI) tract through Notch signaling.

Results and Discussion

Increased Notch activity in the inflamed colonic epithelium

Notch signaling is a major pathway dictating absorptive and secretory cellular differentiation. High Notch activity is observed in the crypts of the inflamed colon of UC patients[18,19]. UC patients also show decreased *ATOH1* expression as well as decreased goblet cell numbers and mucus[5]. CD also shows a similar loss of secretory cells[17]. In mice, the loss of Notch signaling via genetic or chemical inhibition results in intestinal inflammation[1]. Similar to IBD, *Il10*^{-/-} mice also have reduced goblet cells and mucus[20]. The *Il10*^{-/-} mouse model is representative of chronic, immune-mediated intestinal inflammation as IL-10 polymorphisms confer increased risk to both CD and UC [21,22]. We were interested to see if Notch target genes were upregulated in the inflamed colon of *Il10*^{-/-} mice. Utilizing fecal lipocalin-2 (LCN-2) as a marker of intestinal inflammation[23-26], we observed increased fecal LCN-2 levels in *Il10*^{-/-} mice when compared to control C57BL/6 (B6) mice (**Suppl. Fig. 1 A**) as well as increased IFNγ, IL-17A, and IL-22 production from CD4^{+} T cells isolated from mesenteric lymph nodes (**Suppl. Fig. 1 D-F**). Next, we isolated colonocytes from the inflamed colon of *Il10*^{-/-} mice and observed an increase in several Notch target genes including *Hes1*, *Hey1*, and *Dtx1* when compared to the uninflamed colon of control B6 mice (**Fig. 1 A-C**). Although not significantly different from controls, the Notch target gene *Hes5* was trending upwards

(**Fig. 1 D**). Examination of *Gli1*, a gene associated with Hedgehog signaling, another cell determination pathway, showed no change in expression (**Fig. 1 E**). However, when we examined *Atoh1*, a promoter of secretory cells, colonocytes from *Il10*^{-/-} mice showed a significant decrease in *Atoh1* expression compared to the uninflamed colon (**Fig. 1 F**). To determine if this change in Notch activity is due to lack of IL-10 or chronic inflammation, we compared *Hes1* and *Atoh1* expression in an acute and chronic model of dextran sodium sulfate (DSS) induced colitis. Isolated colonocytes from chronic DSS B6 mice showed similar expression patterns of both *Hes1* and *Atoh1* to colitic *Il10*^{-/-} mice (**Suppl. Fig. 1 B, C**). However, colonic *Hes1* and *Atoh1* expression in the acute DSS model were similar to untreated B6 mice (**Suppl. Fig. 1 B, C**). Our data supports prior evidence[5,15-18] of enhanced Notch activity in the colonic epithelium during chronic intestinal inflammation.

Colonic macrophages in the inflamed colon express enhanced levels of Notch ligands. Amassing evidence from IBD patient samples, animal and mathematical models of IBD, as well as identified IBD susceptible risk loci, have all suggested that macrophages are a major cell-type contributing to IBD pathogenesis[5,12-18,27-30]. Given the abundance of macrophages in the gut, we next sought to identify features of colonic macrophages that could contribute to the observed Notch activity in the inflamed colon. As we have previously reported[26], we isolated colonic macrophages from the lamina propria (LP). Similar to what has been observed in the mucosa of IBD patients[13,14], there was an overall increase in the total number of LP macrophages (CX3CR1^{+}MHCII^{+}CD68^{+}) in *Il10*^{-/-} mice compared to controls (**Suppl. Fig. 2 A-C**). A significant portion of these LP macrophages from colitic *Il10*^{-/-} mice expressed Jagged1 compared to macrophages in the non-inflamed gut (**Fig. 2 A, B**). There was also an increase in DLL3^{+} LP macrophages in *Il10*^{-/-} mice (**Fig. 2 C, D**). However, Jagged2, DLL1 and DLL4 expression in macrophages did not show a significant difference between both groups of mice (**Suppl. Fig. 2 D-F**). Lastly, this population of macrophages isolated from colitic mice also showed increased levels of cell surface TLR4 expression (**Suppl. Fig. 2 A, B**) which has been reported to be upregulated during intestinal inflammation[31].

Upon observing that inflammatory macrophages from *Il10*^{-/-} mice show increased Notch ligand expression *in vivo*, we wanted to determine if inflammatory stimuli could upregulate Notch ligand expression in macrophages. Therefore, we generated macrophages from bone marrow monocytes isolated from B6 mice as we have previously described [26,32,33]. Macrophages were stimulated overnight with lipopolysaccharide (LPS) or interferon-gamma (IFNγ) to examine changes in Notch ligand expression. Flow cytometric analysis revealed both LPS and IFNγ stimuli increased expression of Jagged1 **(Fig. 2 E, F).** Under our conditions, these stimuli also increased Jagged2, DLL3 and DLL4 but did not alter DLL1 expression compared to unstimulated macrophages **(Suppl. Fig. 3 A-D)**. Taken together, our data demonstrates an inflammatory microenvironment and signals increase Notch ligand expression in macrophages.

Inflammatory macrophages prevent secretory lineage differentiation

At steady state, intestinal macrophages contribute to ISC differentiation[10]; however, it is unclear how inflammatory macrophages affect ISC differentiation. We reveal a compelling correlation of increased colonic epithelial Notch activity and Notch ligand expression by colonic macrophages in the inflamed colon of *Il10*^{-/-} mice. One possibility is that the inflamed colon harbor ISC that have enhanced expression of Notch receptors that increases Notch activity. When colonic Lgr5^{+} crypt cells were examined for Notch receptor expression there were no observed differences between the proportion of cells expressing Notch receptors (Notch1-4) in the inflamed and uninflamed crypt (**Suppl. Fig. 4 A-E**). This suggest an increase in Notch ligand expression in Notch signal-sending cell(s) may increase Notch activity in the inflamed colon. Interestingly, Notch-1 and -2 as well as DLL1 and DLL4 have been reported to be the respective key receptors and ligands regulating intestinal homeostasis[34-37]. Given there was no difference in DLL1 and DLL4 expression in macrophages suggest other Notch ligand-positive cells contribute to Notch signaling during homeostatic conditions.

We next wanted to examine the impact of macrophage-mediated Notch signaling on colonic ISC differentiation. To do so, we set-up a co-culture system[38] (**Fig. 3**) allowing colonic intestinal stem cells to differentiate in the presence of anti-inflammatory

or inflammatory macrophages. Transwells were seeded with ISC derived from B6 colonoids to form a monolayer. After reaching confluency, monolayers were cultured with either anti-inflammatory (unstimulated, **Fig. 3 A4, C4**) or inflammatory (IFNγ stimulated, **Fig. 3 A5, C5**) macrophages on the basolateral side of the transwell. As shown in **Fig. 2 E** and **Suppl. Fig. 3A-D**, inflammatory macrophages express high levels of Notch ligands. ISC monolayers co-cultured with anti-inflammatory macrophages showed a significant increase in goblet cells as stained by Muc2 (**Fig. 3 A2**) and enteroendocrine cells marked by chromogranin A (CHGA) (**Fig. 3 C2**) when compared to control monolayers with no macrophages (**Fig. 3 A1, C1**). On the other hand, monolayers cultured with inflammatory macrophages inhibited goblet (**Fig. 3 A3, B**) and enteroendocrine cell (**Fig. 3 C3, D**) differentiation. Upon quantification, both goblet and enteroendocrine cells increased by two folds upon co-culture with anti-inflammatory macrophages while there was a slight decrease in goblet cells and no change in enteroendocrine cells upon co-culture with inflammatory macrophages **(Fig. 3 B, D)**. The effect of inflammatory macrophages on the barrier appeared surprisingly similar to monocultures; however, monolayers cultured with inflammatory macrophages showed changes in phalloidin (**Fig. 3 A3, C3**) staining. Although not the scope of this study, in the future we will examine how inflammatory macrophages impact epithelial maturation.

Intestinal macrophages are close to the epithelial barrier, performing tissue remodeling and producing soluble factors such as prostaglandin E_2 and Wnt ligands to maintain the integrity of the barrier[39-42]. CX3CL1-producing epithelial cells and CX3CR1-expression in intestinal macrophages mediate this tissue localization[43-45]. Other studies have utilized macrophage (U937) and colonic epithelial (Caco-2 and HT29) cell lines and shown similar results. U937 cells were skewed to inflammatory cells expressing Notch ligands and were able to turn on Notch in both Caco-2 and HT29 cell lines[46]. Although these are differentiated cell lines and cannot commit to lineage differentiation this suggests inflammatory macrophages are likely to impact the mature epithelium. Taken together, our data demonstrates anti-inflammatory (low Notch ligand expression) macrophages enhance secretory lineage differentiation while inflammatory macrophages (high Notch ligand expression) inhibit secretory lineage differentiation.

Notch activation inhibit secretory lineage differentiation in human colonoids

Inflammatory macrophages produce proinflammatory cytokines[47] (i.e., TNFα, IL-12, IL-23, and IL-1) that can activate inflammatory cells, increase intestinal permeability by dysregulating tight junction proteins as well as induce apoptosis in epithelial cells[48-58]. Notably, these cytokines are the current targets for biological therapy and are at the forefront of IBD treatment. Organoids derived from UC patients show defective goblet cell and mucus production and TNFα was shown to exacerbate this phenotype [59]. In our co-culture studies, inflammatory macrophages were washed before co-culturing but we cannot rule out the effects of cytokines produced during our *in vitro* experiments. Therefore, we wanted to directly assess the role of Notch activation on goblet and enteroendocrine cell development in human colonoids. Human colonoids were allowed to differentiate for 6 days while media was replenished every 48 hrs. During this period, Notch signaling was activated in colonoids using Yhhu3792 (5-(3-Methoxyphenoxy)-N2-[4-(1-methylethyl) phenyl]-2,4-quinazo-linediamine hydrochloride)[60] or inhibited using SAHM1, a modified peptide that disrupts protein-protein interactions and prevents notch complex assembly[61]. Using RNAscope and confocal imaging, we confirmed that Notch activation led to upregulation of the Notch target *HEY1* (**Fig. 4 A, B**) while decreasing the expression of secretory genes *MUC2* (**Fig. 4 C, D**) and *CHGA* (**Fig. 4 E, F**). Interestingly, there was no change in secretory lineage expression upon Notch inhibition when comparing unstimulated colonoids (**Fig. 4 A-F**); however, there was a significant change in secretory marker expression between Notch activation and Notch inhibition (**Fig. 4 B, D, F**). Taken together, this supports our co-culture system that Notch activation on ISC prevents secretory cell development.

Previous reports in IBD patient samples identified Notch activity in different compartments of the epithelium (*i.e.,* Notch activity in crypts and differentiated cells)[5,46]. The loss of Notch signaling via genetic or chemical inhibition results in intestinal inflammation and constitutive Notch signaling is found in IBD and GI cancers. Pan-Notch inhibitors being utilized for cancers are also associated with GI toxicity, specifically, goblet cell hyperplasia[1]. Nevertheless, it is unclear what component of the Notch pathway contributes to intestinal disease or what cell(s) contributes to continuous

Notch activation. Here, we show in a model of intestinal inflammation and ISC differentiation, inflammatory macrophages have increased expression of Notch ligands that can prevent goblet and enteroendocrine cell differentiation (**Suppl. Fig. 5**). Changes in enteroendocrine cell numbers as well as hormones and peptides (both increased and decreased) have been noted in UC and CD, but the mechanism(s) driving these changes are largely unknown. This study suggests Notch signaling from pro-inflammatory macrophages plays a role in enteroendocrine cell changes during intestinal inflammation. Given that additional cells such as dendritic cells and monocytes express Notch ligands we cannot rule out the influence of these cells on ISC differentiation during intestinal inflammation. Additionally, the Notch pathway also promotes proinflammatory T cell activity and can also dampen regulatory T cell function, which could drive IBD pathogenesis [15,62-68]. The interaction of Notch ligand-positive inflammatory macrophages with T cells could also prove problematic for IBD patients. Overall, dysregulated Notch signaling appears to perturb intestinal homeostasis on multiple fronts. Future work will entail understanding the signals of anti-inflammatory macrophages impacting ISC and how inflammatory (Notch ligand-positive) macrophages affect immune cells in the gut.

Methods

Animals

B6.129P2-$Il10^{tm1Cgn}$/J mutant ($Il10^{-/-}$) (002251) and C57BL/6J (000664) mice were purchased from JAX. Both female and male mice between 14-18 weeks of age were used for experiments. All experiments were approved by the Institutional Animal Care and Use Committee of the University of New Mexico Health Sciences Center (IACUC # 20-201025-HSC), in accordance with the National Institutes of Health guidelines for use of live animals. The University of New Mexico Health Sciences Center is accredited by the American Association for Accreditation of Laboratory Animal Care.

Macrophage-Epithelial Co-culture

Crypt isolation and colonoid generation was done as previously reported[69] utilizing proximal colon tissue from B6 mice. Briefly, colonic tissue was minced into 0.5 cm

pieces and washed several times in cold freshly prepared complete chelating solution (CCS; 5.6mM Na2HPO4, 96.2mM NaCl, 1.6mM KCl, 8mM KH2PO4, 43.4mM sucrose, 0.5mM DL-dithiothreitol and 54.9mM D-sorbitol). Colonic tissue was incubated for one hour in 10 mM EDTA in CCS on an orbital shaker at 4°C. Supernatant containing crypts were collected and centrifuged at 1500rpm for 10 minutes at 4°C. Crypts were resuspended in Matrigel (Corning, Tewksbury, MA) and plated in 24-well plates (Corning) as 30 µl droplets or utilized for flow cytometry. After polymerization at 37°C, 500 µl of expansion media (EM), described in supplemental material) was added to each well. Media was replenished every 48 hours. All colonoid cultures were maintained at 37°C with 5% CO_2 and passaged every 5 days. To seed Transwells (0.4 µM pore size), colonoids were harvested from Matrigel using Cultrex Organoid Harvesting Solution as previously described[70]. Colonoids were resuspended in 500 µl of 0.25% trypsin, washed and transferred to 24 well plates. The plates were placed in a spinoculator at 37°C and rocked at 600 rpm for 45 minutes to digest the colonoids into single cells. Digested colonoids were transferred into 15ml conical tubes, containing 10ml PBS and spun down to pellet the cells. The supernatant was removed and single cells were resuspended in 100 µl of filter media and transferred onto collagen-coated Transwells (described in supplemental material). Seeded Transwells were placed in 24 well plates and 600 µl of filter media was added to the bottom of the plate. Both the apical and basal media were replenished every 48 hours until the monolayers were 80-90% confluent. To seed the confluent layer with macrophages, Transwells were carefully flipped utilizing sterile forceps and ensuring the media inside the Transwell did not pour out. Macrophages were generated as described in supplemental material and previously reported[26,33] and resuspended in filter media at a density of 2000 macrophages per microliter. Macrophages suspended in filter media (50 µl) were carefully added to the bottom of the filter to cover the entire surface. The plate was carefully transferred to a cell culture incubator at 37°C for two hours. After, the Transwells were reinserted into the wells of a 24 well plate. Fresh base media (600 µl) to allow for differentiation was added to the bottom of the well while 100 µl was added into the apical side of the Transwell. The co-culture was left for 48 hours at 37°C with 5% CO_2. The apical and basal media was removed, and the monolayer and

macrophages were rinsed twice with PBS, fixed with 4% paraformaldehyde and immunostained (**Suppl. Tables S1 and S4**) for confocal microscopy.

Human Tissue Collection and Human Colonoid Generation

Human colonoid studies were reviewed and approved by the Johns Hopkins University School of Medicine Institutional Review Board (IRB# NA_00038329) and University of New Mexico Institutional Review Board (IRB# 18-171). Colonic biopsies were obtained from healthy individuals undergoing screening colonoscopies who had given informed written consent. Colonic crypt isolation and colonoid generation were prepared as previously reported [69,71]. Briefly, biopsy tissue was minced, washed several times in freshly prepared cold chelating solution (CCS; 5.6mM Na_2HPO_4, 8mM KH_2PO_4, 96.2mM NaCl, 1.6mM KCl, 43.4mM sucrose, 54.9mM D-sorbitol, and 0.5mM DL-dithiothreitol) and incubated 1 hour at 4°C in 10 mM EDTA in CCS on an orbital shaker. Isolated crypts were resuspended in Matrigel (Corning) and 30 μl droplets were plated in a 24-well plate (Corning). After polymerization at 37°C, 500 μl of expansion media (EM) was added for 2 days (Advanced Dulbecco's modified Eagle medium/Ham's F-12 (ThermoFisher, Waltham, MA), 100 U/mL penicillin/streptomycin (Quality Biological, Gaithersburg, MD), 10 mM HEPES (ThermoFisher), and 1X GlutaMAX (ThermoFisher), with 0.15 nM WNT surrogate-Fc fusion protein (ImmunoPrecise Antibodies, Fargo, ND), 15% v/v R-spondin1 conditioned medium (cell line kindly provided by Calvin Kuo, Stanford University), 10% v/v Noggin conditioned medium (cell line kindly provided by Gijs van den Brink, Tytgat Institute for Liver and Intestinal Research), 1X B27 supplement (ThermoFisher), 1 mM N-acetylcysteine (MilliporeSigma), 50 ng/mL human epidermal growth factor (ThermoFisher), 10 nM [Leu-15] gastrin (AnaSpec, Fremont, CA), 500 nM A83-01 (Tocris, Bristol, United Kingdom), 10 μM SB202190 (MilliporeSigma), 100 mg/mL primocin (InvivoGen, San Diego, CA), 10 μM CHIR99021 (Tocris), and 10 μM Y-27632 (Tocris)). After 2 days, the EM (without CHIR99021 and Y-27632) was replaced every other day. Colonoids were passaged every 10-14 days by harvesting in Cultrex Organoid Harvesting Solution (R&D Systems, Minneapolis, MN) at 4°C with shaking for 30'. Colonoids were fragmented by trituration with a P200 pipet 30-50 times, collected and diluted in Advanced DMEM/F12, centrifuged at 300 xg for 10' at

4°C. The pellet was resuspended in Matrigel and plated as described for crypt isolation. All colonoid cultures were maintained at 37°C and 5% CO2. Unless noted, colonoid lines have been passaged >20 times.

RNAscope

RNA was stained in colonoids via the RNAscope protocol (ACD, Newark, CA),with minor changes, as previously described[70]. Briefly, colonoids were harvested from Matrigel and fixed onto lysine coated glass slides with 4% paraformaldehyde for 1 hour. Colonoids were permeabilized with hydrogen peroxide for 10 minutes. Slides were washed 3 times with distilled water, RNAscope Protease Plus was added to submerge the colonoids. Slides were incubated for 30 minutes at 40°C in a humidified tray. Probe hybridization was done for 2 hours at 40°C. Signal amplification and detection were done as described in the RNAscope protocol. Nuclei were stained with DAPI and FluorSave Reagent (Calbiochem) was used to mount coverslips onto the slides. Images were acquired at the UNM AIM Center using the LSM 900 Zeiss AXIO Observer.Z1/7 Inverted Fluorescence Microscope with 63x oil objective lens. Images were processed using the Zen blue (version 3.4) software and ImageJ (version1.8.0) for quantification. All RNA probes used are listed in supplemental table S1.

Statistical Analysis

Statistical analysis was performed as described in figure legends and graphs generated display mean (± SD or SEM) and were obtained using GraphPad Prism software. The data were analyzed using one-way ANOVA or two-tailed unpaired Student's t test (Prism).

Online supplemental material. Material and methods for colitis induction, cell and tissue preparation, organoid media, RT-qPCR, flow cytometry, ELISA, and immunostaining are found in supplemental material.

Author contributions. RA performed all experiments and analysis with the help from ASR, AJM, SDM, JGI, and EFC. JGI participated in imaging and analysis and provided

reagents for organoids. RA, ASR, and JGI participated in writing the manuscript. EFC designed the study, analyzed data and wrote the paper. All authors approved the final version of the manuscript.

Declaration of Competing Interest

The authors declare no conflict of interest.

Acknowledgments

References

1   Demitrack, E. S. & Samuelson, L. C. Notch regulation of gastrointestinal stem cells. *J Physiol* **594**, 4791-4803, doi:10.1113/JP271667 (2016).

2   Kopan, R. & Ilagan, M. X. The canonical Notch signaling pathway: unfolding the activation mechanism. *Cell* **137**, 216-233, doi:10.1016/j.cell.2009.03.045 (2009).

3   Tsai, Y. H. *et al.* ADAM10 regulates Notch function in intestinal stem cells of mice. *Gastroenterology* **147**, 822-834 e813, doi:10.1053/j.gastro.2014.07.003 (2014).

4   Ueo, T. *et al.* The role of Hes genes in intestinal development, homeostasis and tumor formation. *Development* **139**, 1071-1082, doi:10.1242/dev.069070 (2012).

5   Zheng, X. *et al.* Suppression of hath1 gene expression directly regulated by hes1 via notch signaling is associated with goblet cell depletion in ulcerative colitis. *Inflamm Bowel Dis* **17**, 2251-2260, doi:10.1002/ibd.21611 (2011).

6   VanDussen, K. L. *et al.* Notch signaling modulates proliferation and differentiation of intestinal crypt base columnar stem cells. *Development* **139**, 488-497, doi:10.1242/dev.070763 (2012).

7   VanDussen, K. L. & Samuelson, L. C. Mouse atonal homolog 1 directs intestinal progenitors to secretory cell rather than absorptive cell fate. *Dev Biol* **346**, 215-223, doi:10.1016/j.ydbio.2010.07.026 (2010).

8   Shroyer, N. F. *et al.* Intestine-specific ablation of mouse atonal homolog 1 (Math1) reveals a role in cellular homeostasis. *Gastroenterology* **132**, 2478-2488, doi:10.1053/j.gastro.2007.03.047 (2007).

9   Yang, Q., Bermingham, N. A., Finegold, M. J. & Zoghbi, H. Y. Requirement of Math1 for secretory cell lineage commitment in the mouse intestine. *Science* **294**, 2155-2158, doi:10.1126/science.1065718 (2001).

10   Sehgal, A. *et al.* The role of CSF1R-dependent macrophages in control of the intestinal stem-cell niche. *Nat Commun* **9**, 1272, doi:10.1038/s41467-018-03638-6 (2018).

11   Bain, C. C. *et al.* Constant replenishment from circulating monocytes maintains the macrophage pool in the intestine of adult mice. *Nat Immunol* **15**, 929-937, doi:10.1038/ni.2967 (2014).

12   Bain, C. C. *et al.* Resident and pro-inflammatory macrophages in the colon represent alternative context-dependent fates of the same Ly6Chi monocyte precursors. *Mucosal Immunol* **6**, 498-510, doi:10.1038/mi.2012.89 (2013).

13   Bernardo, D. *et al.* Human intestinal pro-inflammatory CD11c(high)CCR2(+)CX3CR1(+) macrophages, but not their tolerogenic CD11c(-)CCR2(-)CX3CR1(-) counterparts, are expanded in inflammatory bowel disease. *Mucosal Immunol* **11**, 1114-1126, doi:10.1038/s41385-018-0030-7 (2018).

14   Kamada, N. *et al.* Unique CD14 intestinal macrophages contribute to the pathogenesis of Crohn disease via IL-23/IFN-gamma axis. *J Clin Invest* **118**, 2269-2280, doi:10.1172/JCI34610 (2008).

15   Dahan, S. *et al.* Notch-1 signaling regulates intestinal epithelial barrier function, through interaction with CD4+ T cells, in mice and humans. *Gastroenterology* **140**, 550-559, doi:10.1053/j.gastro.2010.10.057 (2011).

16   Wehkamp, J. *et al.* Reduced Paneth cell alpha-defensins in ileal Crohn's disease. *Proc Natl Acad Sci U S A* **102**, 18129-18134, doi:10.1073/pnas.0505256102 (2005).

17   Gersemann, M. *et al.* Differences in goblet cell differentiation between Crohn's disease and ulcerative colitis. *Differentiation* **77**, 84-94, doi:10.1016/j.diff.2008.09.008 (2009).

18   Okamoto, R. *et al.* Requirement of Notch activation during regeneration of the intestinal epithelia. *Am J Physiol Gastrointest Liver Physiol* **296**, G23-35, doi:10.1152/ajpgi.90225.2008 (2009).

19   Ghorbaninejad, M. *et al.* Contribution of NOTCH signaling pathway along with TNF-alpha in the intestinal inflammation of ulcerative colitis. *Gastroenterol Hepatol Bed Bench* **12**, S80-S86 (2019).

20   Johansson, M. E. *et al.* Bacteria penetrate the normally impenetrable inner colon mucus layer in both murine colitis models and patients with ulcerative colitis. *Gut* **63**, 281-291, doi:10.1136/gutjnl-2012-303207 (2014).

21   Shouval, D. S. *et al.* Interleukin-10 receptor signaling in innate immune cells regulates mucosal immune tolerance and anti-inflammatory macrophage function. *Immunity* **40**, 706-719, doi:10.1016/j.immuni.2014.03.011 (2014).

22   Kuhn, R., Lohler, J., Rennick, D., Rajewsky, K. & Muller, W. Interleukin-10-deficient mice develop chronic enterocolitis. *Cell* **75**, 263-274, doi:10.1016/0092-8674(93)80068-p (1993).

23   Playford, R. J. *et al.* Effects of mouse and human lipocalin homologues 24p3/lcn2 and neutrophil gelatinase-associated lipocalin on gastrointestinal mucosal integrity and repair. *Gastroenterology* **131**, 809-817, doi:10.1053/j.gastro.2006.05.051 (2006).

24   Alpizar-Alpizar, W. *et al.* Neutrophil gelatinase-associated lipocalin (NGAL/Lcn2) is upregulated in gastric mucosa infected with Helicobacter pylori. *Virchows Arch* **455**, 225-233, doi:10.1007/s00428-009-0825-8 (2009).

25   Raffatellu, M. *et al.* Lipocalin-2 resistance confers an advantage to Salmonella enterica serotype Typhimurium for growth and survival in the inflamed intestine. *Cell Host Microbe* **5**, 476-486, doi:10.1016/j.chom.2009.03.011 (2009).

26   Merkley, S. D. *et al.* Non-autophagy Role of Atg5 and NBR1 in Unconventional Secretion of IL-12 Prevents Gut Dysbiosis and Inflammation. *J Crohns Colitis* **16**, 259-274, doi:10.1093/ecco-jcc/jjab144 (2022).

27   Na, Y. R., Stakenborg, M., Seok, S. H. & Matteoli, G. Macrophages in intestinal inflammation and resolution: a potential therapeutic target in IBD. *Nature reviews. Gastroenterology & hepatology* **16**, 531-543, doi:10.1038/s41575-019-0172-4 (2019).

28   Zigmond, E. *et al.* Ly6C hi monocytes in the inflamed colon give rise to proinflammatory effector cells and migratory antigen-presenting cells. *Immunity* **37**, 1076-1090, doi:10.1016/j.immuni.2012.08.026 (2012).

29   Zigmond, E. *et al.* Macrophage-restricted interleukin-10 receptor deficiency, but not IL-10 deficiency, causes severe spontaneous colitis. *Immunity* **40**, 720-733, doi:10.1016/j.immuni.2014.03.012 (2014).

30   Wendelsdorf, K., Bassaganya-Riera, J., Hontecillas, R. & Eubank, S. Model of colonic inflammation: immune modulatory mechanisms in inflammatory bowel disease. *J Theor Biol* **264**, 1225-1239, doi:10.1016/j.jtbi.2010.03.027 (2010).

31   Hausmann, M. *et al.* Toll-like receptors 2 and 4 are up-regulated during intestinal inflammation. *Gastroenterology* **122**, 1987-2000, doi:10.1053/gast.2002.33662 (2002).

32   Castillo, E. F. *et al.* Autophagy protects against active tuberculosis by suppressing bacterial burden and inflammation. *Proc Natl Acad Sci U S A* **109**, E3168-3176, doi:10.1073/pnas.1210500109 (2012).

33   Merkley, S. D. *et al.* Polystyrene microplastics induce an immunometabolic active state in macrophages. *Cell Biol Toxicol*, doi:10.1007/s10565-021-09616-x (2021).

34   Pellegrinet, L. *et al.* Dll1- and dll4-mediated notch signaling are required for homeostasis of intestinal stem cells. *Gastroenterology* **140**, 1230-1240 e1231-1237, doi:10.1053/j.gastro.2011.01.005 (2011).

35   van Es, J. H., de Geest, N., van de Born, M., Clevers, H. & Hassan, B. A. Intestinal stem cells lacking the Math1 tumour suppressor are refractory to Notch inhibitors. *Nat Commun* **1**, 18, doi:10.1038/ncomms1017 (2010).

36   Fre, S. *et al.* Notch signals control the fate of immature progenitor cells in the intestine. *Nature* **435**, 964-968, doi:10.1038/nature03589 (2005).

37   Riccio, O. *et al.* Loss of intestinal crypt progenitor cells owing to inactivation of both Notch1 and Notch2 is accompanied by derepression of CDK inhibitors p27Kip1 and p57Kip2. *EMBO Rep* **9**, 377-383, doi:10.1038/embor.2008.7 (2008).

38   Noel, G. *et al.* A primary human macrophage-enteroid co-culture model to investigate mucosal gut physiology and host-pathogen interactions. *Sci Rep* **7**, 45270, doi:10.1038/srep45270 (2017).

39   Tessner, T. G., Muhale, F., Riehl, T. E., Anant, S. & Stenson, W. F. Prostaglandin E2 reduces radiation-induced epithelial apoptosis through a mechanism involving AKT activation and bax translocation. *J Clin Invest* **114**, 1676-1685, doi:10.1172/JCI22218 (2004).

40   Brown, S. L. *et al.* Myd88-dependent positioning of Ptgs2-expressing stromal cells maintains colonic epithelial proliferation during injury. *J Clin Invest* **117**, 258-269, doi:10.1172/JCI29159 (2007).

41   Kaler, P., Godasi, B. N., Augenlicht, L. & Klampfer, L. The NF-kappaB/AKT-dependent Induction of Wnt Signaling in Colon Cancer Cells by Macrophages and IL-1beta. *Cancer Microenviron* **2**, 69-80, doi:10.1007/s12307-009-0030-y (2009).

42   Cosin-Roger, J., Ortiz-Masia, M. D. & Barrachina, M. D. Macrophages as an Emerging Source of Wnt Ligands: Relevance in Mucosal Integrity. *Frontiers in immunology* **10**, 2297, doi:10.3389/fimmu.2019.02297 (2019).

43   Kim, K. W. *et al.* In vivo structure/function and expression analysis of the CX3C chemokine fractalkine. *Blood* **118**, e156-167, doi:10.1182/blood-2011-04-348946 (2011).

44   Medina-Contreras, O. *et al.* CX3CR1 regulates intestinal macrophage homeostasis, bacterial translocation, and colitogenic Th17 responses in mice. *J Clin Invest* **121**, 4787-4795, doi:10.1172/JCI59150 (2011).

45   Yona, S. *et al.* Fate mapping reveals origins and dynamics of monocytes and tissue macrophages under homeostasis. *Immunity* **38**, 79-91, doi:10.1016/j.immuni.2012.12.001 (2013).

46   Ortiz-Masia, D. *et al.* M1 Macrophages Activate Notch Signalling in Epithelial Cells: Relevance in Crohn's Disease. *J Crohns Colitis* **10**, 582-592, doi:10.1093/ecco-jcc/jjw009 (2016).

47   Neurath, M. F. Current and emerging therapeutic targets for IBD. *Nat Rev Gastroenterol Hepatol* **14**, 269-278, doi:10.1038/nrgastro.2016.208 (2017).

48   Homaidan, F. R., El-Sabban, M. E., Chakroun, I., El-Sibai, M. & Dbaibo, G. S. IL-1 stimulates ceramide accumulation without inducing apoptosis in intestinal epithelial cells. *Mediators Inflamm* **11**, 39-45, doi:10.1080/09629350210313 (2002).

49   Gitter, A. H., Bendfeldt, K., Schulzke, J. D. & Fromm, M. Leaks in the epithelial barrier caused by spontaneous and TNF-alpha-induced single-cell apoptosis. *FASEB J* **14**, 1749-1753, doi:10.1096/fj.99-0898com (2000).

50   Goretsky, T. *et al.* p53 mediates TNF-induced epithelial cell apoptosis in IBD. *Am J Pathol* **181**, 1306-1315, doi:10.1016/j.ajpath.2012.06.016 (2012).

51   Pott, J. & Maloy, K. J. Epithelial autophagy controls chronic colitis by reducing TNF-induced apoptosis. *Autophagy* **14**, 1460-1461, doi:10.1080/15548627.2018.1450021 (2018).

52   Al-Sadi, R. M. & Ma, T. Y. IL-1beta causes an increase in intestinal epithelial tight junction permeability. *J Immunol* **178**, 4641-4649, doi:10.4049/jimmunol.178.7.4641 (2007).

53   Al-Sadi, R., Ye, D., Said, H. M. & Ma, T. Y. IL-1beta-induced increase in intestinal epithelial tight junction permeability is mediated by MEKK-1 activation of canonical NF-kappaB pathway. *Am J Pathol* **177**, 2310-2322, doi:10.2353/ajpath.2010.100371 (2010).

54   Al-Sadi, R., Ye, D., Dokladny, K. & Ma, T. Y. Mechanism of IL-1beta-induced increase in intestinal epithelial tight junction permeability. *J Immunol* **180**, 5653-5661, doi:10.4049/jimmunol.180.8.5653 (2008).

55   Yang, F., Zhao, K., Zhang, X., Zhang, J. & Xu, B. ATP Induces Disruption of Tight Junction Proteins via IL-1 Beta-Dependent MMP-9 Activation of Human Blood-Brain Barrier In Vitro. *Neural Plast* **2016**, 8928530, doi:10.1155/2016/8928530 (2016).

56   Ma, T. Y. *et al.* TNF-alpha-induced increase in intestinal epithelial tight junction permeability requires NF-kappa B activation. *Am J Physiol Gastrointest Liver Physiol* **286**, G367-376, doi:10.1152/ajpgi.00173.2003 (2004).

57   Ma, T. Y., Boivin, M. A., Ye, D., Pedram, A. & Said, H. M. Mechanism of TNF-{alpha} modulation of Caco-2 intestinal epithelial tight junction barrier: role of myosin light-chain kinase protein expression. *Am J Physiol Gastrointest Liver Physiol* **288**, G422-430, doi:10.1152/ajpgi.00412.2004 (2005).

58   Al-Sadi, R., Guo, S., Ye, D., Rawat, M. & Ma, T. Y. TNF-alpha Modulation of Intestinal Tight Junction Permeability Is Mediated by NIK/IKK-alpha Axis Activation of the Canonical NF-kappaB Pathway. *Am J Pathol* **186**, 1151-1165, doi:10.1016/j.ajpath.2015.12.016 (2016).

59   Singh, V. *et al.* Chronic Inflammation in Ulcerative Colitis Causes Long-Term Changes in Goblet Cell Function. *Cell Mol Gastroenterol Hepatol* **13**, 219-232, doi:10.1016/j.jcmgh.2021.08.010 (2022).

60   Lu, H. *et al.* A Novel 2-Phenylamino-Quinazoline-Based Compound Expands the Neural Stem Cell Pool and Promotes the Hippocampal Neurogenesis and the Cognitive Ability of Adult Mice. *Stem Cells* **36**, 1273-1285, doi:10.1002/stem.2843 (2018).

61   Moellering, R. E. *et al.* Direct inhibition of the NOTCH transcription factor complex. *Nature* **462**, 182-188, doi:10.1038/nature08543 (2009).

62   Tsao, P. N. *et al.* Lipopolysaccharide-induced Notch signaling activation through JNK-dependent pathway regulates inflammatory response. *J Biomed Sci* **18**, 56, doi:10.1186/1423-0127-18-56 (2011).

63   Charbonnier, L. M., Wang, S., Georgiev, P., Sefik, E. & Chatila, T. A. Control of peripheral tolerance by regulatory T cell-intrinsic Notch signaling. *Nat Immunol* **16**, 1162-1173, doi:10.1038/ni.3288 (2015).

64   Auderset, F., Coutaz, M. & Tacchini-Cottier, F. The role of Notch in the differentiation of CD4(+) T helper cells. *Curr Top Microbiol Immunol* **360**, 115-134, doi:10.1007/82_2012_227 (2012).

65   Alam, M. S. *et al.* Notch signaling drives IL-22 secretion in CD4+ T cells by stimulating the aryl hydrocarbon receptor. *Proc Natl Acad Sci U S A* **107**, 5943-5948, doi:10.1073/pnas.0911755107 (2010).

66   Sauma, D., Ramirez, A., Alvarez, K., Rosemblatt, M. & Bono, M. R. Notch signalling regulates cytokine production by CD8+ and CD4+ T cells. *Scand J Immunol* **75**, 389-400, doi:10.1111/j.1365-3083.2012.02673.x (2012).

67   Xu, H. *et al.* Notch-RBP-J signaling regulates the transcription factor IRF8 to promote inflammatory macrophage polarization. *Nat Immunol* **13**, 642-650, doi:10.1038/ni.2304 (2012).

68   Palaga, T. *et al.* Notch signaling is activated by TLR stimulation and regulates macrophage functions. *European journal of immunology* **38**, 174-183, doi:10.1002/eji.200636999 (2008).

69   In, J. *et al.* Enterohemorrhagic Escherichia coli reduce mucus and intermicrovillar bridges in human stem cell-derived colonoids. *Cell Mol Gastroenterol Hepatol* **2**, 48-62 e43, doi:10.1016/j.jcmgh.2015.10.001 (2016).

70   Atanga, R., Parra, A. S. & In, J. G. Efficient RNA and RNA-protein co-detection in 3D colonoids by whole-mount staining. *STAR Protoc* **3**, 101775, doi:10.1016/j.xpro.2022.101775 (2022).

71   Jung, P. *et al.* Isolation and in vitro expansion of human colonic stem cells. *Nat Med* **17**, 1225-1227, doi:10.1038/nm.2470 (2011).
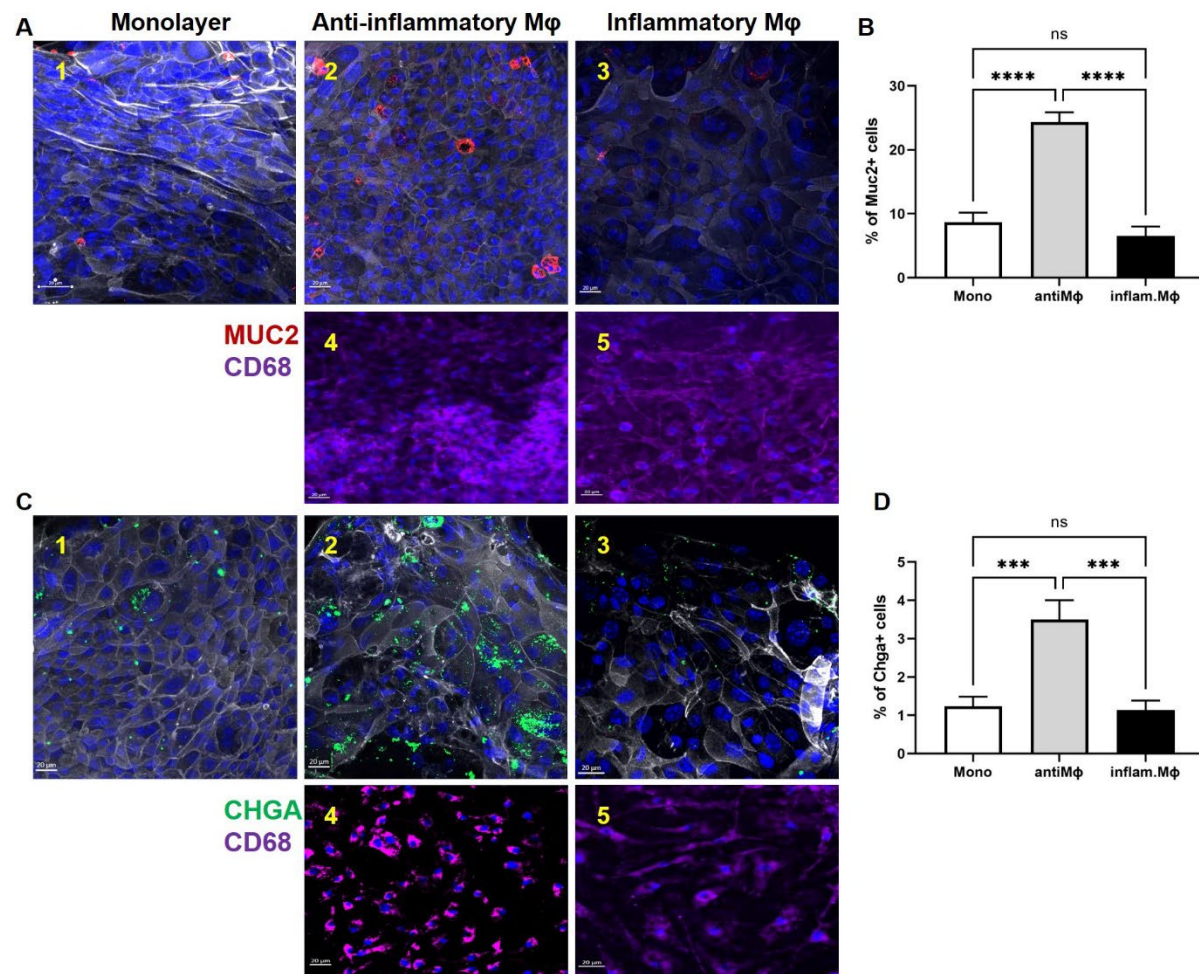
Figure 1
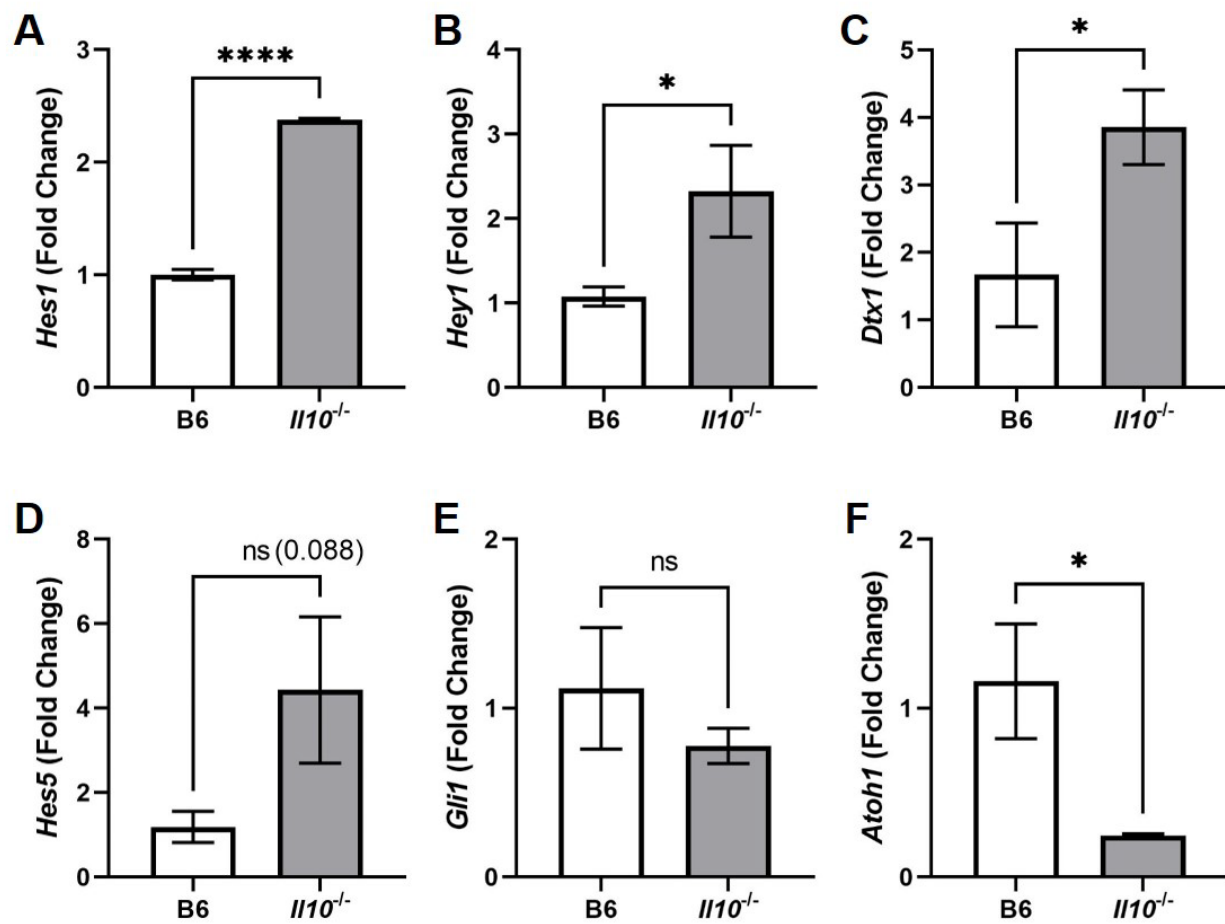
Figure 1. Notch target gene expression in the colon of *Il10^{-/-}* mice. mRNA expression of **(A)** *Hes1*, **(B)** *Hey1*, **(C)** *Dtx1*, **(D)** *Hes5*, **(E)** *Gli1*, and **(F)** *Atoh1* in the inflamed colon of *Il10^{-/-}* mice compared to the uninflamed colon of (B6) mice. Two independent experiments, n = 8/group. Graphs indicate mean (±SEM). * P<0.05, ****P<0.0001, ns, not significant. Significance was calculated by two-tailed unpaired Student's t test.

Figure 2
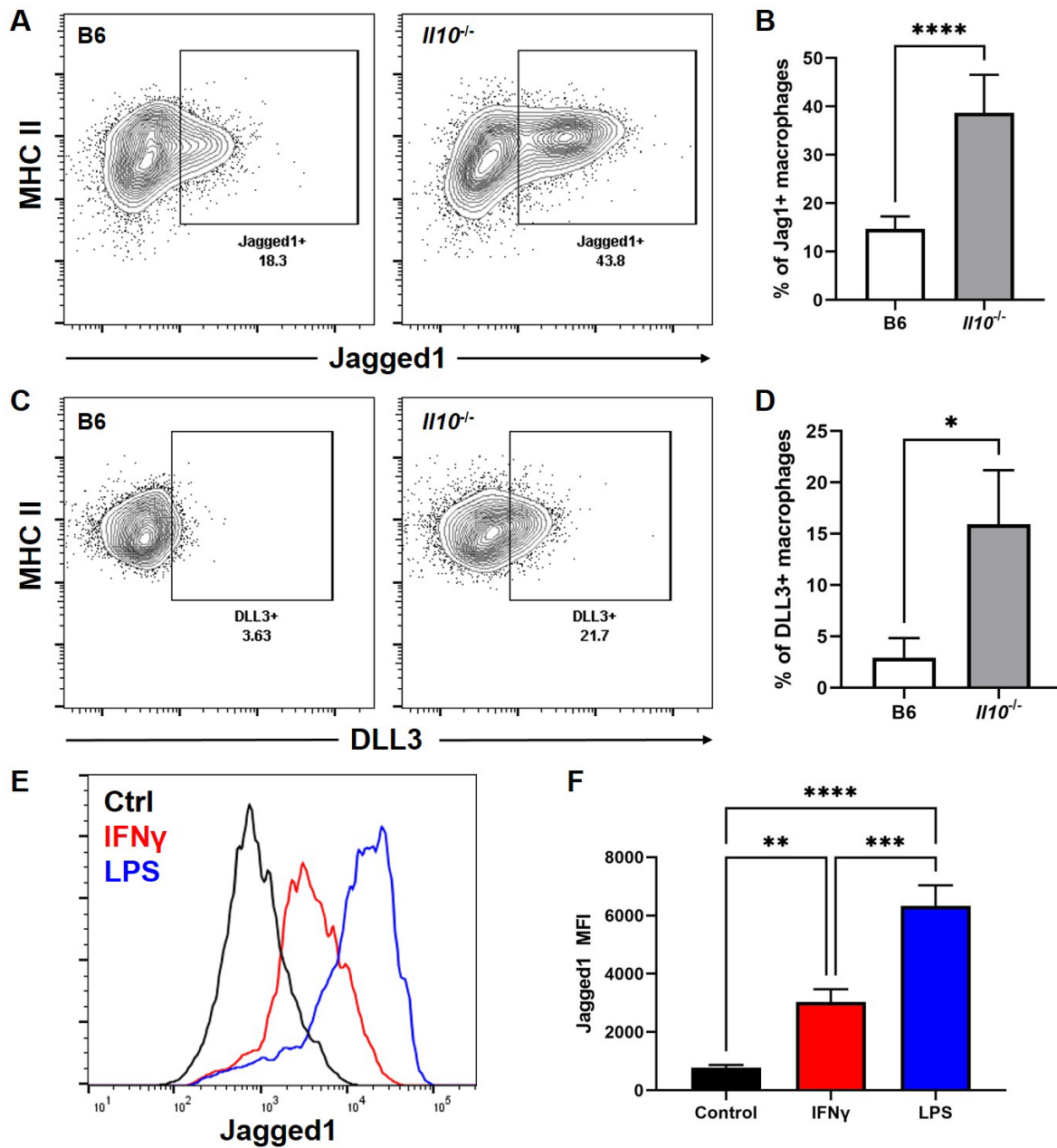
Figure 2. Notch ligand expression in lamina propria macrophages. Phenotype of lamina propria macrophages in colitic *Il10*$^{-/-}$ mice. **(A)** Representative flow cytometric plots showing MHC II and Jagged1 expression in LP macrophages (gated on CD45$^+$MHC-II$^+$CX3CR1$^+$CD68$^+$ cells) isolated from colitic *Il10*$^{-/-}$ mice and non-colitic B6 mice. **(B)** Graph showing percent of Jagged1$^+$ (Jag1) LP macrophages from both group of mice. **(C)** Representative flow cytometric plots showing MHC II and DLL3 expression in LP macrophages isolated from colitic *Il10*$^{-/-}$ mice and non-colitic B6 mice. **(D)** Graph showing percent of DLL3$^+$ LP macrophages from both group of mice. **(E)** Representative histogram showing Jagged1 expression in B6 macrophages stimulated with LPS (Blue) or IFNγ (Red) compared to baseline/unstimulated (Black) macrophages. **(F)** Graph showing the geometric mean fluorescence intensity (MFI) of Jagged1 on unstimulated and stimulated B6 macrophages. Representative of two independent experiments, Graphs indicate mean (±SD). * P<0.05, **P<0.01, ***P<0.001, ****P<0.0001. Significance was calculated by two-tailed unpaired Student's t test or one-way ANOVA.
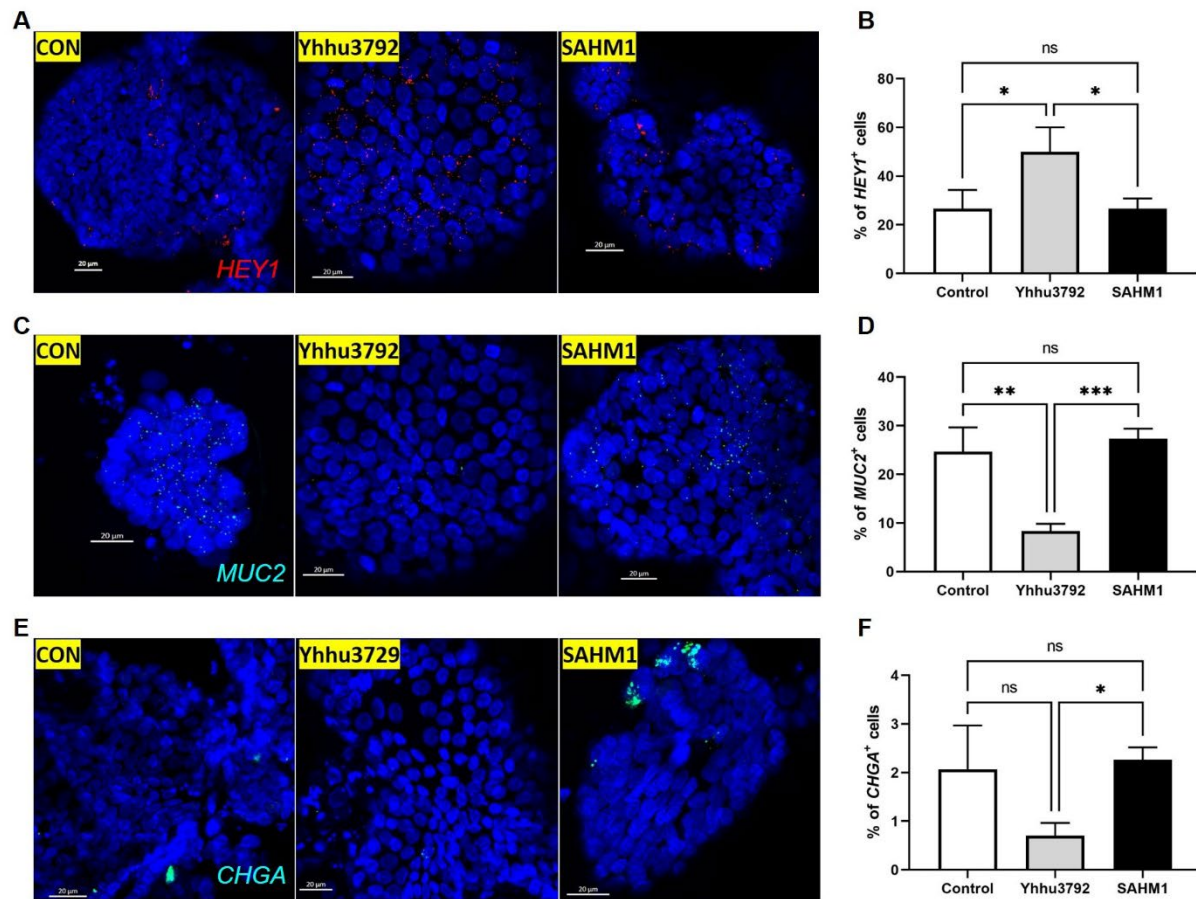
Figure 3

Figure 3. Inflammatory macrophages inhibit secretory lineage differentiation. Representative images showing mucin 2 (MUC2) and chromogranin A (CHGA) detection in mouse epithelia-macrophage (CD68) co-cultures after ISC differentiation. **(A)** MUC2 (Red) staining in 1) epithelial monolayers, 2) co-culture with anti-inflammatory macrophages (Mφ), 3) co-culture with inflammatory macrophages, 4 and 5) staining of CD68 (Purple) on the basolateral surface. **(B)** Graph shows the proportion of MUC2$^+$ cells out of 1000 cells counted in each condition. **(C)** CHGA (Green) staining in 1) epithelial monolayers, 2) co-culture with anti-inflammatory macrophages (Mφ), 3) co-culture with inflammatory macrophages, 4 and 5) staining of CD68 (purple) on the basolateral surface. **D)** Graph shows the proportion of CHGA$^+$ cells out of 1000 cells counted in each condition. Representative of two independent experiments, n=3 per group. Graphs indicate mean (±SD). ***P<0.001, ****P<0.0001, ns, not significant. Significance was calculated by one-way ANOVA.

Figure 4

Figure 4. Notch activation decrease secretory lineage marker expression in human colonoids. Macrophage-free Notch activation in Human colonoids. Colonoids were treated with 10 µM of the Notch activator Yhhu3792 or 40 µM of the Notch inhibitor SAHM1 for 6 days. Notch target *HEY1* and secretory lineage markers *MUC2* and *CHGA* were quantified via RNA scope. **(A)** RNAscope detection of *HEY1* in human colonoids after left untreated or treated with Yhhu3792, or SAHM1. **(B)** Graph shows the proportion of *HEY1*+ cells out of 1000 cells counted in each condition. **(C)** RNAscope detection of *MUC2* in human colonoids after left untreated or treated with Yhhu3792, or SAHM1. **(D)** Graph shows the proportion of *MUC2*+ cells out of 1000 cells counted in each condition. **(E)** RNAscope detection of *CHGA* in human colonoids after left untreated or treated with Yhhu3792, or SAHM1. **(F)** Graph shows the proportion of *CHGA*+ cells out of 1000 cells counted in each condition. Representative of two independent experiments, n=3 per group. Graphs indicate mean (±SD). * $P<0.05$, **$P<0.01$, ***$P<0.001$, ns, not significant. Significance was calculated by one-way ANOVA.

Inflammatory macrophages prevent colonic goblet and enteroendocrine cell differentiation through Notch signaling

Roger Atanga *et al.*,

Supplementary Methods and References, Supplemental Tables (1-4), Supplemental Figures and Figure Legends (1-5).

Supplementary Methods

Colitis

Il10^{-/-} mice showed early inflammatory changes by 10-12 weeks after weaning and more severe inflammation by 14-16 weeks. Dextran Sodium Sulfate (DSS, colitis grade, ~30,000 -50,000 MW; MP Biomedicals) was used for both acute and chronic DSS-induced colitis in C57BL/6J female mice between 8-16 weeks of age. In the acute model, mice were provided 2.5% DSS in drinking water ad-libitum for 7 days and then switched to drinking water for 7 days. In the chronic model, mice received three cycles of 2.5% DSS in drinking water ad-libitum for 7 days and each cycle was separated with two weeks of drinking water. Stool was utilized to detect lipocalin-2 (LCN-2). Stool samples were weighed and diluted in 0.1% PBS-Tween. LCN-2 ELISA was performed using Quantikine ELISA Kits (R&D Systems) according to the manufacturer's specifications.

Cells and tissue preparation. Colonic epithelial cells and lamina propria (LP) macrophages were isolated from the colon by a three-step process [1-3]. 1) Separation of the colonic epithelium from the LP by chelation using 2 mM EDTA and 0.5mM dithiothreitol in HBSS buffer; 2) digestion of the remaining colon with collagenase and dispase; and 3) enrichment of CD45^{+} cells using biotinylated CD45 antibody and streptavidin beads from the digested fraction. Colonic epithelial cells were cryopreserved in RNA-Later (Invitrogen) for RNA isolation. LP macrophages were used for flow cytometric analysis. Mesenteric lymph nodes (mLN) were collected and manually homogenized into single cell suspensions. mLN cells were resuspended in RPMI prior to plating and then stimulated with phorbol 12-myristate 13-acetate (PMA,

50 ng/mL) and Ionomycin (500 ng/mL) in the presence of Brefeldin A/GolgiPlug (1:1000, BD Biosciences) and Monesin/GolgiStop, (1:1000, BD Biosciences) in preparation for intracellular cytokine staining and analysis by flow cytometry.

Generation of primary macrophages

The generation of primary macrophages were prepared as briefly described [3,4], marrow was collected from the femur and tibia, washed and differentiated in DMEM (Gibco), FBS (VWR), and murine L929-fibroblast supernatant containing CSF-1 for 10 days, after which cellular morphology was evaluated to confirm differentiation. Macrophages were rested for 16 hours in media without CSF-1 prior to stimulation with LPS (200 ng/mL, Thermofisher) or IFNγ (10 ng/mL, Peprotech) overnight. Macrophages were used for flow cytometric analysis or co-culturing with epithelial cells derived from organoids. Prior to co-culturing with colonic epithelial cells, macrophages were washed twice before incubation.

Flow Cytometry

Bone marrow-derived or LP cells were pretreated with Stain FcX (anti-CD16/32) (Biolegend) before being stained for cell surface markers. For staining, cells were washed with FACS buffer [90% by volume 1x PBS, (Life Technologies), 10%FBS (VWR), and 0.05% 0.5 M EDTA, (Invitrogen)] prior to staining. Cells were incubated for 20 min with antibody stain in FACS buffer, followed by washing with FACS buffer, and fixation in 1% PFA. To examine intracellular proteins, cells were permeabilized and incubated with antibodies targeting cytokines for 30 minutes and then washed and resuspended in FACS buffer. Sample analysis was performed on LSR Fortessa (BD Biosciences) and analyzed using FlowJo software (TreeStar). Antibodies used for flow cytometric analysis are listed in Table S2.

RNA Isolation, Quantification, and RT-qPCR

RNA isolation was performed on cells or tissues cryopreserved in RNA-Later (Invitrogen) using the RNA Purelink Minikit (Invitrogen) according to the manufacturer's protocols. RNA was quantified on Nanodrop2000 and all samples yielded a 260/280 of 2 ± 0.15. cDNA synthesis was performed using Oligo(dT) Primer and SSIV Reverse

Transcriptase in the presence of Cloned Ribonuclease Inhibitor (all ThermoFisher). Reverse transcription reaction and RT-qPCR runs utilized Taqman MasterMix (ThermoFisher) on a viiA7 Thermal Cycler (ThermoFisher) using QuantStudio 7. RT-qPCR primers and reagents used are listed in Table S3.

Immunostaining for Confocal Microscopy

Colonoids were harvested from Matrigel using Cultrex Organoid Harvesting Solution as previously described[5]. Colonoids were fixed for 30 minutes in 4% paraformaldehyde (Electron Microscopy Sciences, Hatfield, PA). Colonoids were washed twice using 500 µl of 1X PBS. Colonoids were permeabilized and blocked simultaneously for 1 hour using a 10% Fetal Bovine Serum (Atlanta Biologicals, Flowery Branch, GA), 0.1% saponin (MilliporeSigma) solution prepared in PBS. After permeabilization, colonoids were washed three times in 1X PBS. 100 µl of primary antibody prepared at 1:50 dilution in 1X PBS was added to organoids and incubated overnight at 4°C. Organoids were washed 3 times with 1X PBS, and 100 µl of AlexaFluor secondary antibodies including AlexaFluor-647 phalloidin, diluted 1:200 in 1X PBS, were added for 1h at room temperature. Hoechst 33342 (ThermoFisher) 1 mg/ml was added for 5 minutes. After three 1X PBS washes, FluorSave Reagent (Calbiochem) was added to the colonoids and mounted on glass slides. Confocal imaging was performed at the UNM AIM Center using the LSM 900 Zeiss AXIO Observer Z1/7 Inverted Fluorescence Microscope. Images were processed using the Zen blue (version 3.4) software. Images were processed using the Zen blue (version 3.4). Primary and secondary antibodies used are listed on Table S4.

Organoid Growth media

Intestinal organoid media for monolayer plating (referred to as 'filter media') was comprised of Advanced Dulbecco's modified Eagle medium/Ham's F-12 (ThermoFisher, Waltham, MA), 100 U/mL penicillin/streptomycin (Quality Biological, Gaithersburg, MD), 50% v/v WNT3A conditioned medium (ATCC CRL-2647), 15% v/v R-spondin1 conditioned medium (cell line kindly provided by Calvin Kuo, Stanford University), 10% v/v Noggin conditioned medium (cell line kindly provided by Gijs van den Brink, Tytgat Institute for Liver and Intestinal Research), 1X B27 supplement (ThermoFisher), 10 mM HEPES (ThermoFisher), 1X GlutaMAX (ThermoFisher), 1mM N-acetylcysteine

(MilliporeSigma), 50 ng/mL human epidermal growth factor (ThermoFisher), 10 nM [Leu-15] gastrin (AnaSpec, Fremont, CA), 500 nM A83-01 (Tocris, Bristol, United Kingdom), 10 µM SB202190 (MilliporeSigma), 100 mg/mL primocin (InvivoGen, San Diego, CA). Intestinal organoid media for expansion of 3-dimensional organoids (referred to as expansion media) had the same composition as filter media except for the replacement of 50% v/v WNT3A conditioned medium with 0.15 nM WNT surrogate-Fc fusion protein (ImmunoPrecise Antibodies, Fargo, ND). The volume of the conditional WNT3A was made up for by Advanced Dulbecco's modified Eagle medium/Ham's F-12 (ThermoFisher). Base media, for differentiation of organoids, had the same composition of filter media but lacked WNT3A, Rspo-1 and SB202190. 0.4 µM pore sizeTranswell filters (Corning) were coated using 100 µl of 100 µg rat collagen IV (Corning) at 4°C overnight, aspirated, and washed (3x) with 200 µl of sterile water prior to use.

References

1   Ray, A. L. *et al.* Blockade of MK2 is protective in inflammation-associated colorectal cancer development. *Int J Cancer* **138**, 770-775, doi:10.1002/ijc.29716 (2016).
2   Stonier, S. W., Ma, L. J., Castillo, E. F. & Schluns, K. S. Dendritic cells drive memory CD8 T-cell homeostasis via IL-15 transpresentation. *Blood* **112**, 4546-4554, doi:10.1182/blood-2008-05-156307 (2008).
3   Merkley, S. D. *et al.* Non-autophagy Role of Atg5 and NBR1 in Unconventional Secretion of IL-12 Prevents Gut Dysbiosis and Inflammation. *J Crohns Colitis* **16**, 259-274, doi:10.1093/ecco-jcc/jjab144 (2022).
4   Castillo, E. F. *et al.* Autophagy protects against active tuberculosis by suppressing bacterial burden and inflammation. *Proc Natl Acad Sci U S A* **109**, E3168-3176, doi:10.1073/pnas.1210500109 (2012).
5   Atanga, R., Parra, A. S. & In, J. G. Efficient RNA and RNA-protein co-detection in 3D colonoids by whole-mount staining. *STAR Protoc* **3**, 101775, doi:10.1016/j.xpro.2022.101775 (2022).

Supplemental Tables

Table S1. RNAScope probes

Probe	Source	Identifier
Hs-CHGA-C4	ACD	Cat# 311111-C4
Hs-HEY1	ACD	Cat# 311201
Hs-MUC2-c2	ACD	Cat# 3122871-C2

Table S2. Flow Cytometry antibodies

Antibody	Conjugate	Company	Catalog #
CD45	eFluor 450	eBioscience	48-0451-82
MHC II	APC-eFluor780	eBioscience	47-5321-82
CD68	Brilliant Violet 605	BioLegend	137021
CX3CR1	Brilliant Violet 510	BioLegend	149025
TLR4/MD2	PE-Cyanine7 (PE-Cy7)	eBioscience	25-9924-82
Jagged1	Phycoerythrin (PE)	eBioscience	12-3391-82
Jagged2	eFluor 660	Invitrogen	50-3392-82
DLL1	Alexa Fluor 488	Invitrogen	1942873
DLL3	PE	BioLegend	154004
DLL4	APC	BioLegend	130814
CD4	PE-Cy7	Invitrogen	25-0041-82
TCRβ	FITC	Invitrogen	11-5961-82
IFNγ	PE	eBioscience	12-7311-82
IL-17A	eFluor 660	eBioscience	50-7177-82
IL-22	PerCP-eFluor710	eBioscience	46-7222-82
Lgr5	PE	Origene	TA400001
Lgr5	Alexa Fluor 647	R&D Systems	FAB8240R
EpCAM	eFluor 450	eBioscience	48-5791-82
c-Kit/CD117	Alexa Fluor 700	BioLegend	105826
CD24	PerCP-Cy5.5	Invitrogen	45-0242-80
Notch1	APC	Invitrogen	17-5765-82
Notch2	PE	Invitrogen	12-5786-82
Notch3	Alexa Fluor 647	BioLegend	130512
Notch4	PE	BioLegend	128407
CD45	Biotin	BioLegend	103104

**Table S3. PCR Primers**

Assay ID	Source	Identifier
Atoh1: Mm00476035_s1	ThermoFisher	Cat# 4331182
Gapdh: Mm99999915_	ThermoFisher	Cat# 4331182
Hes1: Mm01342805_m1	ThermoFisher	Cat# 4331182
Hey1: Mm00468865_m1	ThermoFisher	Cat# 4453320
Hes5: Mm00439311_g1	ThermoFisher	Cat# 4331182
Dtx1: Mm00492297_m1	ThermoFisher	Cat# 4453320
Gli5: Mm00494654_m1	ThermoFisher	Cat# 4331182

Table S4. Primary and secondary antibodies for Immunostaining

Antibody	Source	Identifier
CD68	ThermoFisher	Cat# 140681-82
MUC2	Novus	Cat# NBP1 31231
Chromogranin A	Santa Cruz	Cat# Sc393941
Donkey anti-Rabbit IgG-AF488	ThermoFisher	Cat# A-21206
Donkey anti-Mouse IgG, AF568	ThermoFisher	Cat# A10037
Donkey anti-Mouse IgG, AF488	ThermoFisher	Cat# A21202
Goat anti-Rabbit IgG AF568	ThermoFisher	Cat# A1101042
Phalloidin-Alexa Fluor 647	AAT Bioquest	Cat# 1000854

Supplemental Figure 1
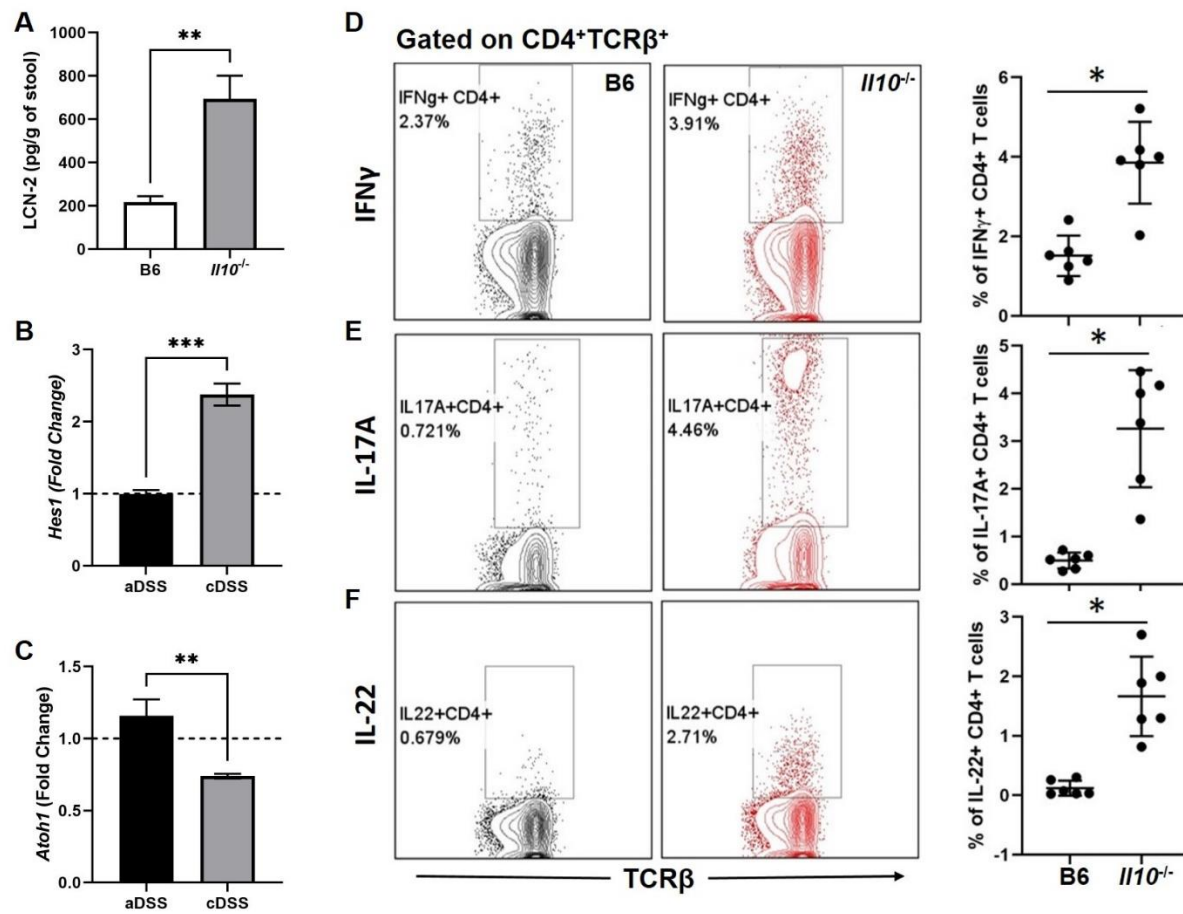
Supplemental Figure 1. Comparison of colitic *Il10⁻/⁻* and non-colitic B6 mice. (A)
Fecal LCN-2 levels as detected by ELISA from colitic *Il10⁻/⁻* and non-colitic B6 mice.
Colon epithelial **(B)** *Hes1* and **(C)** *Atoh1* gene expression after acute (aDSS) and
chronic (cDSS) DSS-induced colitis. **(D)** Representative dot plots showing Intracellular
IFNγ staining in CD4⁺ T cells isolated from mLN in colitic *Il10⁻/⁻* and non-colitic B6 mice
and corresponding graph. **(E)** Representative dot plots showing Intracellular IL-17A
staining in CD4⁺ T cells isolated from mLN in colitic *Il10⁻/⁻* and non-colitic B6 mice and
corresponding graph. **(F)** Representative dot plots showing Intracellular IL-22 staining in
CD4⁺ T cells isolated from mLN in colitic *Il10⁻/⁻* and non-colitic B6 mice and
corresponding graph. Representative of two independent experiments, Graphs indicate
mean (±SEM). *P<0.05, **P<0.01, ***P<0.001, Significance was calculated by two-tailed
unpaired Student's t test.

Supplemental Figure 2
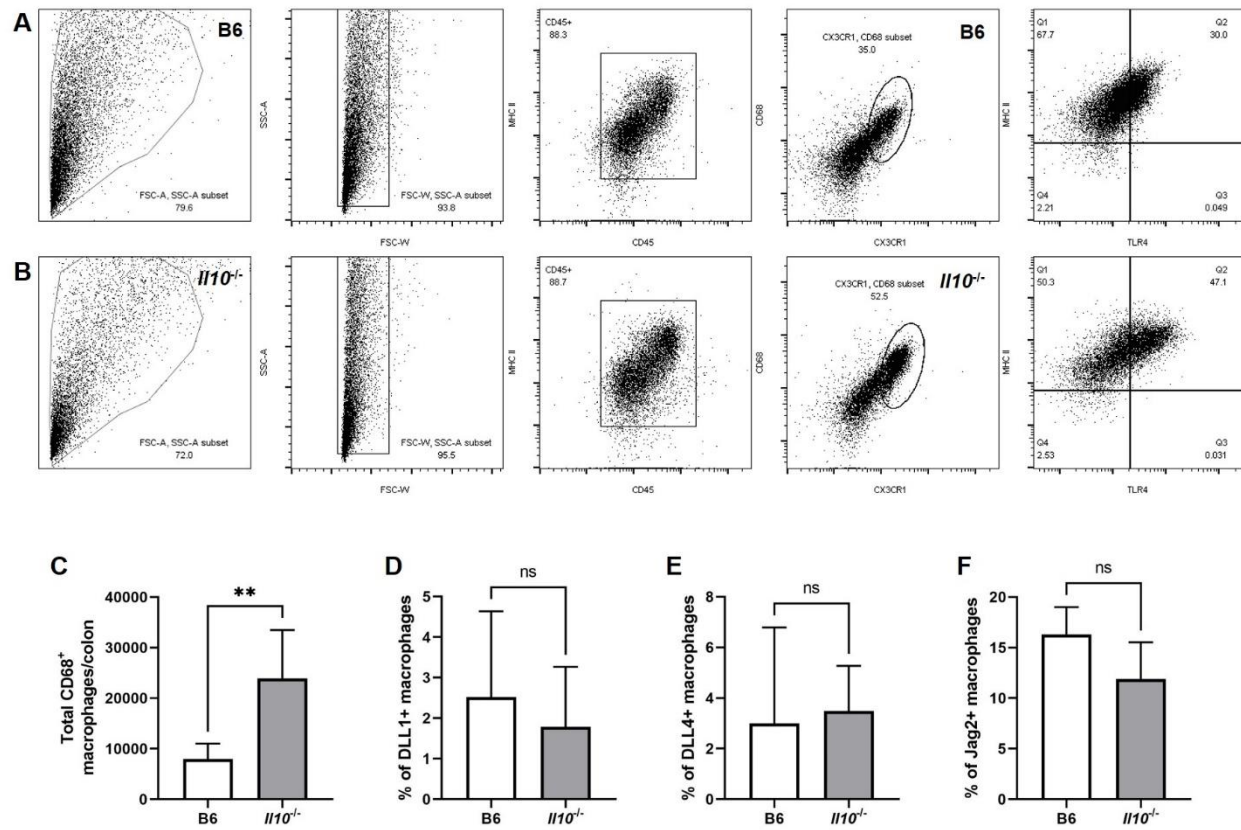
**Supplemental Figure 2. Colonic lamina propria macrophages and Notch ligand expression.** Gating strategy of LP macrophages from **(A)** B6 and **(B)** *Il10$^{-/-}$* mice. **(A, B)** Dot plots showing FSC/SSC. FSC-W and lamina propria (gated on CD45$^+$ and MHC II$^+$) cells and further gated on CD68 and CX3CR1. Dot plot showing gated CD68+ cells TLR4 expression. **(C)** Graph showing total number of macrophages (MHC-II$^+$CD68$^+$CX3CR1$^+$). **(D-F)** Graphs showing the percent of **(D)** DLL1$^+$, **(E)** DLL4$^+$, and **(F)** Jagged2$^+$ (Jag2) macrophages. Representative of two independent experiments (n=3 per group), Graphs indicate mean (±SD). **P<0.01, ns, not significant. Significance was calculated by two-tailed unpaired Student's t test.

Supplemental Figure 3
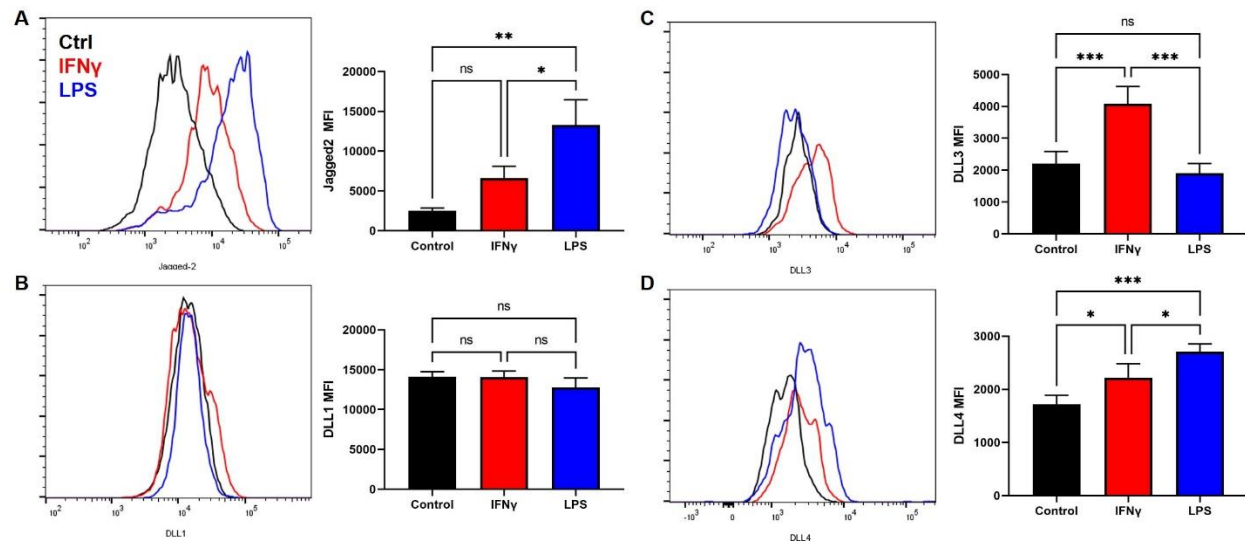
Supplemental Figure 3. Notch ligand expression in macrophages after inflammatory stimulation. Representative histograms showing **(A)** Jagged2, **(B)** DLL1, **(C)** DLL3, and **(D)** DLL4 expression in B6 macrophages stimulated with LPS (Blue) or IFNγ (Red) compared to baseline/unstimulated (Black) macrophages and corresponding graph showing the geometric mean fluorescence intensity (MFI) of **(A)** Jagged2, **(B)** DLL1, **(C)** DLL3, and **(D)** DLL4 in unstimulated and stimulated B6 macrophages. Representative of two independent experiments (n=3 per group), Graphs indicate mean (±SD). *P<0.05, **P<0.01, ***P<0.001, ns, not significant. Significance was calculated by one-way ANOVA.
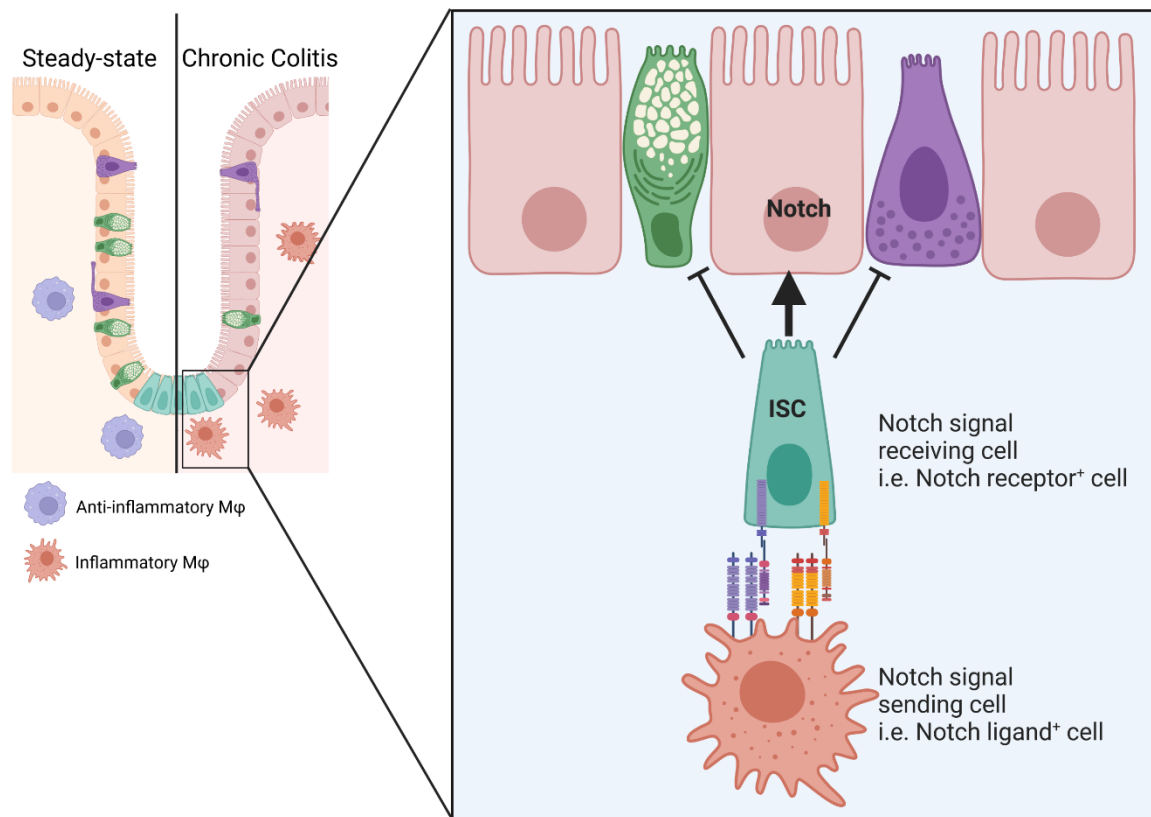
Supplemental Figure 4
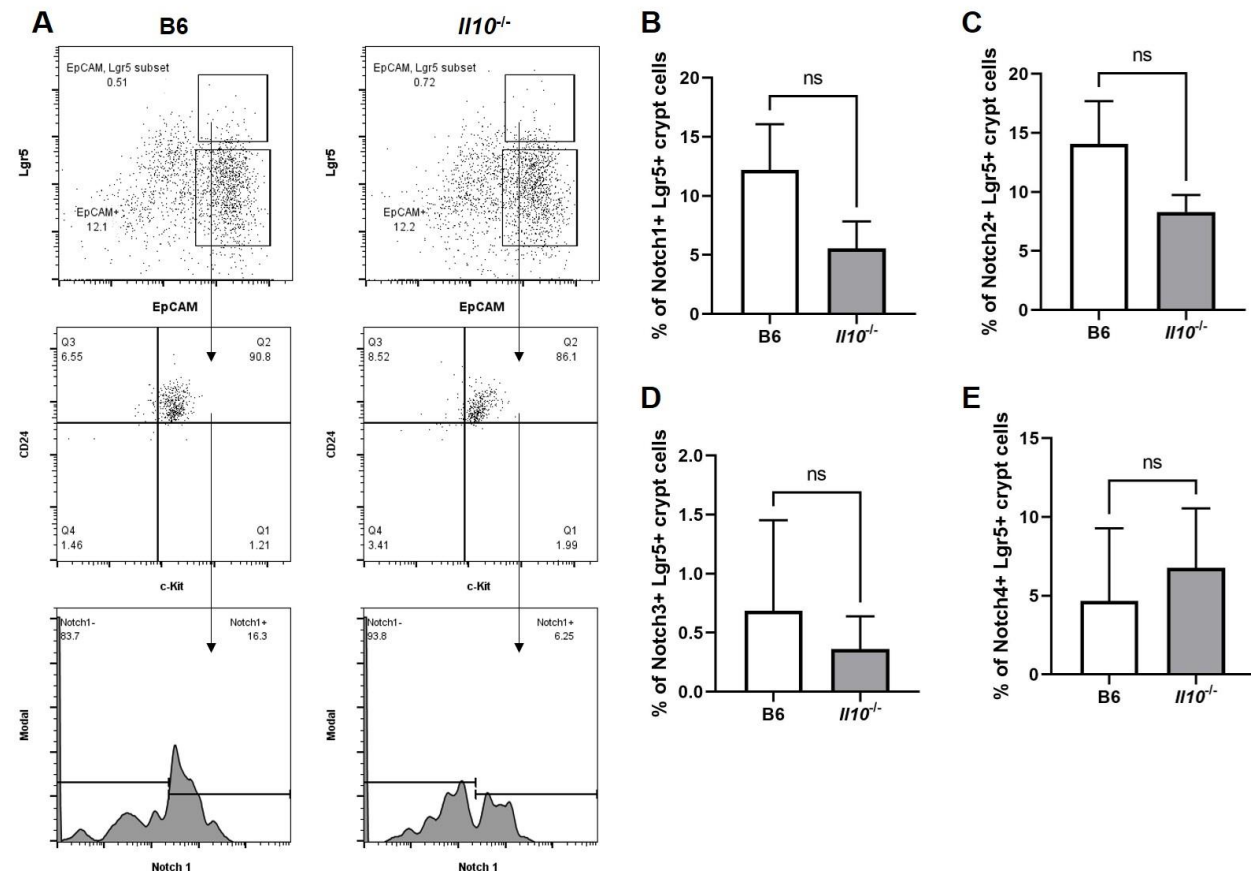
Supplemental Figure 4. Notch Receptor on colonic crypt cells. Crypt cells were isolated from the colon of B6 or *Il10*$^{-/-}$ mice to examine Notch receptor expression. **(A)** Gating strategy of Lgr5$^+$ crypt cells – Lgr5$^+$ EpCAM$^+$CD24$^+$c-Kit$^+$ cells were examined for Notch receptor expression. Graphs showing the percent of **(B)** Notch1, **(C)** Notch2, **(D)** Notch3, and **(E)** Notch4 Lgr5$^+$ crypt cells isolated from B6 or *Il10*$^{-/-}$ mice. Representative of two independent experiments (n=3 per group), Graphs indicate mean (±SD). ns, not significant. Significance was calculated by two-tailed unpaired Student's t test.

Supplemental Figure 5

Supplemental Figure 5. Graphical image showing inflammatory macrophages express increased levels of Notch ligands that can influence intestinal stem cells (ISC) to become absorptive cells through the promotion of Notch signaling (Image made with BioRender).